energies

MDPI

Article

A Fast State Estimator for Integrated Electrical and Heating Networks

Chun Wang [1], Minghao Geng [2], Qingshan Xu [1,*] and Haixiang Zang [2]

[1] School of Electrical Engineering, Southeast University, Nanjing 210096, China; 230188174@seu.edu.cn
[2] College of Energy and Electrical Engineering, Hohai University, Nanjing 210098, China; gengmhhhu@163.com (M.G.); zanghaixiang@hhu.edu.cn (H.Z.)
* Correspondence: xuqingshan@seu.edu.cn; Tel.: +86-138-1383-7607

Received: 17 July 2020; Accepted: 27 August 2020; Published: 31 August 2020

Abstract: Integrated electrical and heating networks (IEHNs) effectively improve energy utilization efficiency, reduce environmental pollution and realize sustainable development of energy. To realize the accurate, comprehensive and fast perception of the integrated electrical and heating networks, it is necessary to build a state estimation model. However, the robust state estimator of IEHNs based on the temperature drop equation, flow balance equation and power balance equation still have the problems of convergence and low computational efficiency. In this paper, a fast state estimation method based on weighted least absolute value is proposed, which makes partition calculation of ring-shaped heating network and radiant heating network under certain assumptions. Simulation results show that the method improves the efficiency of the robust state estimator on the premise of high accuracy.

Keywords: integrated electrical and heating networks; state estimation; weighted least squares absolute value

1. Introduction

The increasingly prominent problems of energy and environment have promoted the change of energy consumption patterns of human beings. How to improve energy utilization efficiency, reduce environmental pollution and realize sustainable development of energy is a topic of common concern today [1,2]. Thus, the integrated energy system is considered as the main form of energy in the future [3,4]. Among them, the integrated electrical and heating networks (IEHNs) centered on combined heat and power (CHP) can produce electric energy and available heat at the same time (Figure 1), which have great flexibility [5]. At present, the research on IEHNs mainly focuses on system modeling, planning, scheduling, optimization and evaluation [6–12]. However, online scheduling execution and control policy specification depend on complete and reliable real-time data, which is often limited or inaccurate for technical reasons. Therefore, in order to realize the comprehensive, real-time and accurate perception of the operation status of IEHNs, it is urgent to study the SE (state estimation) method for IEHNs.

The current research on state estimation of IEHNs is still in the initial stage. In [13], an SE method for calculating heat energy loss was proposed. [14] proposed a weighted least square (WLS) state estimation method for IEHNs, which has high convergence and can obtain high estimation accuracy in the absence of bad data. It has important theoretical significance and application value. Sheng et al. [15] proposed an extended IEHN model that also considered the dynamics of pipelines, and applied a two-stage SE approach to solve the model. Zhang [16] developed a decentralized algorithm based on the asynchronous alternating direction method of multipliers for integrated heat and power networks, in which the measurement information between the two networks is not shared. In [17], the state

estimation model with the full heating network constraints of IEHNs was established, and a robust state estimation method based on a pseudo-measurement model was proposed. [18] proposed a bilinear, weighted least absolute value (WLAV) SE method for IEHNs. Sheng proposed a two-stage iterative hybrid state estimation method for integrated heat and electricity networks [19]. Through this method, the time delay of thermal transportation is considered and estimated. The case study shows that the hybrid state estimator using this method has good performance in both stable and dynamic processes. Zheng proposed a distributed state estimation method for cogeneration systems [20]. This method can also be used to handle communication failures. Case studies have proved the effectiveness and advantages of the distributed state estimation method. However, the WLAV state estimation algorithm of IEHNs based on the temperature drop equation, flow balance equation and power balance equation still have the problems of convergence and low computational efficiency. The problem of robust estimation efficiency has been solved in an integrated electricity-gas system by a bilinear model proposed by Chen [21,22] and traditional SE for power system [23].

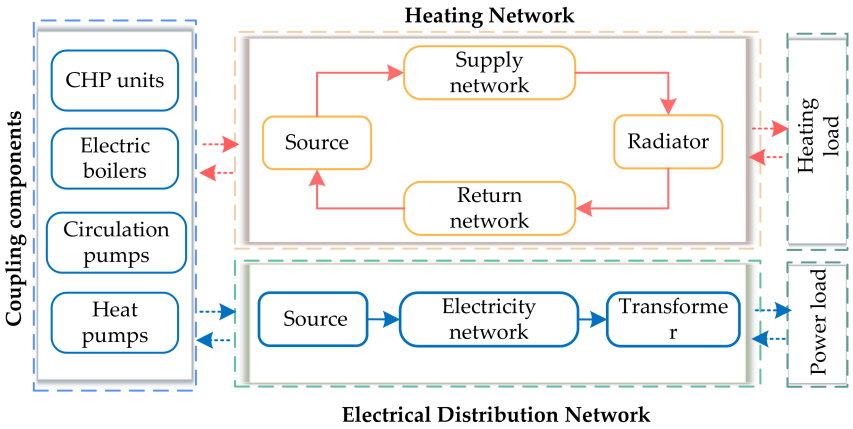

Figure 1. Schematic illustrating the structure of an integrated electrical and heating network (IEHN).

The present work seeks to address these research gaps by a fast state estimation method of IEHNs-based WLAV for IEHN presented in this paper.

1. Firstly, in the modeling and analysis of heating network, the heat network pipeline is divided into a ring-shaped heating network and radiant heating network. Under the assumption that the heating temperature and backwater temperature have little change in the actual heating network, the temperature and mass flow rate are decoupled to carry out in the state estimator of radiant heating network.
2. In this paper, the state estimation of heating network is carried out from a distributed point of view. Boundary state constraints are set on the boundary of the ring-shaped heating network and radiant heating network. This method can improve the efficiency of IEHNs state estimation by simplifying the calculation scale of the ring-shaped heating network.

2. State Estimation Model for IEHNs

The IEHNs considered in this paper is composed of the electricity subsystem, the heat subsystem and various coupling units such as CHPs and circulation pumps. The electricity subsystem is described by the AC power flow model; the heat subsystem is described by the static model, which consists of heat sources, heat loads, supply and return water pipelines.

2.1. Objective Function

WLAV has great significance in the state estimation for IEHNs—because of the working environment and automation level of thermal meters, the possibility of bad data in measurement of

heating network is often higher than that in electrical network [24]. The objective of the WLAV criterion is to minimize the weighted sum of absolute values of the differences between the actual measurements and the estimated ones. The mathematical model of WLAV state estimation with equality constraints is as follows:

$$\begin{aligned} \min\ & J(x) = w_e^T|\varepsilon_e| + w_h^T|\varepsilon_h| \\ s.t\quad & \varepsilon_e = z_e - h_x(x_e) \\ & \varepsilon_h = z_h - h_h(x_h) \\ & c(x) = 0 \end{aligned} \tag{1}$$

where $x = [x_e^T, x_e^T]^T$ is the state variables of IEHN.

In the electricity subsystem, the state vector is denoted by $x_e = [V, \theta]^T$, where V is the nodal voltage magnitudes and θ is the voltage phase angles. The main types of measurement are branch power, node injection power and node voltage magnitude, which can be denoted by $z_e = [P_{ij}^{meas}, Q_{ij}^{meas}, P_i^{meas}, Q_i^{meas}, V_i^{meas}]^T$.

As for the heat subsystem measurements, the state vector is denoted by $x_h = [m, T_s, T_r]^T$, where m is the mass flow rates and T_s, T_r are the supply and return temperature. Measurements include the mass flow rates of pipelines, mass flow through each node injected from a source or discharged to a load, pressure head losses within a pipe, heat power consumed at load node or the useful heat output of CHP units, supply temperature and return temperature, summarized by the vector $z_h = [m^{meas}, m_q^{meas}, h_f^{meas}, \Phi^{meas}, T_s^{meas}, T_r^{meas}]^T$.

$c(x)$ are the constraint equations in the IEHN, which can be divided into four sections: power constraints, thermal constraints, hydraulic constraints and coupling constraints.

2.2. Constraints Equation

2.2.1. Power Constraints

The zero-injections constraint in the electricity subsystem can be denoted by:

$$\begin{cases} P_i = real\left\{V(YV)^*\right\} = 0 \\ Q_i = imag\left\{V(YV)^*\right\} = 0 \end{cases} \tag{2}$$

2.2.2. Thermal Constraints

As shown in Figure 2, there is a temperature loss between the two adjacent points of the heat network due to the heat transfer process. The temperature loss between nodes is expressed by a complex exponential equation. The temperature drop equation is described in detail in Equation (9) in Section 3. In this paper, the model simplification of the radial heat network is also the simplification of the temperature drop equation. But here, the supply/return temperature mismatches are processed as thermal constraints:

$$\begin{cases} A_s T_s' - b_s = 0 \\ A_r T_r' - b_r = 0 \end{cases} \tag{3}$$

where (A_s, b_s, A_r, b_r) are the matrix of coefficients for brevity. The derivation process is described in detail in reference [7]. The main idea is to separate the constant part of Equation (9) from the variables.

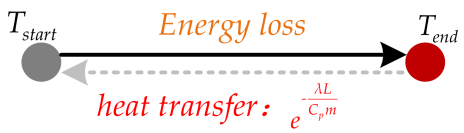

Figure 2. Temperature constraint between two nodes.

2.2.3. Hydraulic Constraints

In the heating network shown in Figure 3, the branch part with the loop network satisfies the loop pressure equation, which is similar to the Kirchhoff voltage law in the power network. The loop pressure constraints should be satisfied [7]:

$$BKm|m| = 0 \tag{4}$$

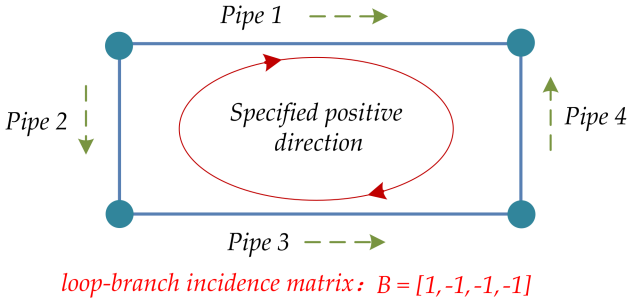

Figure 3. The schematic diagram of loop pressure equation.

Similar to the zero-power injection node in the power grid, there are also zero-injections constraints in the heat subsystem [17]:

$$A_k m = 0 \tag{5}$$

2.2.4. Coupling Component Constraints

The coupling unit constraints can be summarized:

$$P_{CHP} - \zeta \Phi_{CHP} = 0 \tag{6}$$

3. Measurement Model for Heating Network

3.1. Ring-shaped Heating Network Measurement Models

According to the actual measurements in the heating network, the measurement functions are followed:

$$Hydraulic\ Model \begin{cases} m_i = m_i \\ m_{qi} = A \cdot m_i \\ h_{fi} = K \cdot m_i \cdot |m_i| \end{cases} \tag{7}$$

$$Thermal\ Model \begin{cases} \Phi_i = C_p(A \cdot m_i) \cdot (T_{si} - T_{oi}) \\ T_{si} = T_{si} \\ T_{ri} = T_{ri} \\ T_{r\_source,k} = f_h(m_i, T_{ri}) \end{cases} \tag{8}$$

where A is the node-branch incidence matrix and $f_h(\cdot)$ represents the temperature relationship between the two ends of the pipe in the temperature drop equation, which can be described as:

$$T_{end} = (T_{start} - T_a)e^{-\frac{\lambda L}{C_p m}} + T_a \tag{9}$$

where λ is the overall heat transfer coefficient per unit length; L is the pipe length; C_p is the specific heat of water. T_{start} represents the temperature of the node at the beginning of the pipeline and T_{end} represents the temperature of the node at the end of the pipeline.

It can be seen from the Equation (8) that there is a coupling relationship between flow rate and temperature in the measurement equation of the ring-shaped heating network, which increases the calculation amount of the state estimation.

3.2. Radiant Heating Network Measurement Model

Equation (9) contains an exponential equation, the computational complexity is high and the numerical stability is difficult to guarantee. By using two order approximation of Taylor expansion, the temperature drop Equation (9) can be written as:

$$\begin{array}{c} T_{end} = (T_{start} - T_a)e^{-\lambda L/(C_p m)} + T_a \approx \\ (T_{start} - T_a)(1 - \frac{\lambda L}{C_p m} + \frac{1}{2}\frac{\lambda^2 L^2}{C_p^2 m^2}) + T_a \end{array} \tag{10}$$

From (10), the temperature drop equation of pipeline 2 can be described as:

$$T_{s2} = (T_{s1} - T_a)(1 - \frac{\lambda_2 L_2}{C_p m} + \frac{1}{2}\frac{\lambda_2^2 L_2^2}{C_p^2 m^2}) + T_a \tag{11}$$

where T_{s1} is the supply temperature of node 1 in Figure 4, T_{s2} is the supply temperature of node 2 in Figure 4, L_2 and λ_2 is the pipe length and the overall heat transfer coefficient per unit length of pipeline 2, the subscript of the variable represents the number of the pipe or node in Figure 4.

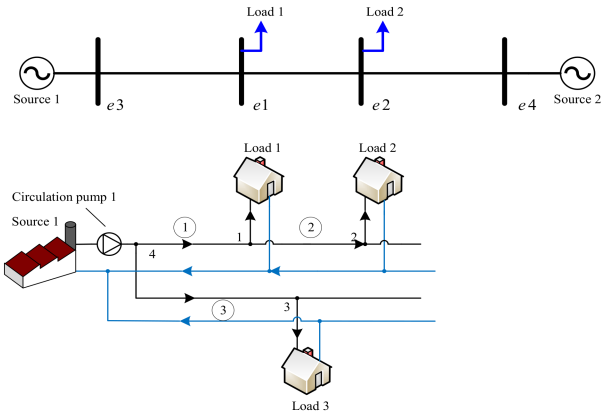

Figure 4. Radiant heating network coupled a simple electricity network (case study 1).

Similarly, for pipeline 1:

$$T_{s1} = (T_{s4} - T_a)(1 - \frac{\lambda_1 L_1}{C_p m} + \frac{1}{2}\frac{\lambda_1^2 L_1^2}{C_p^2 m^2}) + T_a \tag{12}$$

From (10) and (11), we can obtain:

$$\begin{array}{c} T_{s2} = (T_{s4} - T_a)(1 - \frac{\lambda_1 L_1}{C_p m} + \frac{1}{2}\frac{\lambda_1^2 L_1^2}{C_p^2 m^2})\times \\ (1 - \frac{\lambda_1 L_1}{C_p m} + \frac{1}{2}\frac{\lambda_1^2 L_1^2}{C_p^2 m^2}) + T_a \end{array} \tag{13}$$

Since

$$T_{s2} = \Phi_2/(C_p m) + T_{o2} \tag{14}$$

where Φ_2 is the load power consumed by load 2, T_{o2} is the outlet temperature of node 2 before to mixing in the return network.

From (13) and (14), the following expressions are obtained:

$$\frac{\Phi_2}{C_p m} + T_{o2} = (T_{s4} - T_a)(1 - \frac{\lambda_1 L_1}{C_p m} + \frac{1}{2}\frac{\lambda_1^2 L_1^2}{C_p^2 m^2})\times (1 - \frac{\lambda_2 L_2}{C_p m} + \frac{1}{2}\frac{\lambda_2^2 L_2^2}{C_p^2 m^2}) + T_a \quad (15)$$

We can round the C_p^3 and C_p^4 in the denominator to simplify Equation (15):

$$\frac{T_{s4}-T_{o2}}{T_{s4}-T_a} m^2 - [\frac{\lambda_1 L_1 + \lambda_2 L_2}{C_p} + \frac{\Phi_2}{C_p(T_{s4}-T_a)}]m + \frac{(\lambda_1 L_1 + \lambda_2 L_2)^2}{2C_p^2} = 0 \quad (16)$$

Equation (15) may also applied to more pipelines:

$$\frac{T_{s4}-T_{o2}}{T_{s4}-T_a} m^2 - [\frac{\lambda_1 L_1 + \lambda_2 L_2 + \cdots + \lambda_N L_N}{C_p} + \frac{\Phi_2}{C_p(T_{s4}-T_a)}]m + \frac{(\lambda_1 L_1 + \lambda_2 L_2 + \cdots + \lambda_N L_N)^2}{2C_p^2} = 0 \quad (17)$$

However, due to the heating load, the actual pipeline flow rates are not equal, so Equation (16) is an approximate model [25].

4. Proposed Methodology

The framework of the proposed fast state estimation approach of IEHN is represented in Figure 5.

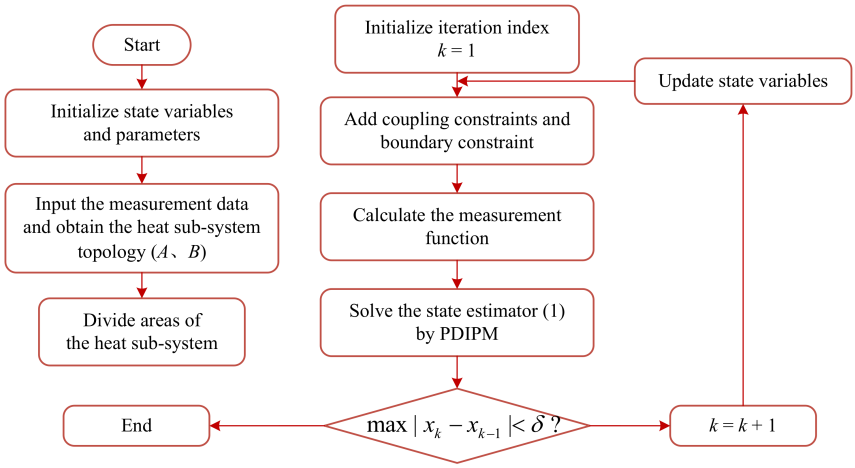

Figure 5. Flowchart of the state estimation approach of IEHN. PDIPM: primal-dual interior point method.

Main steps of the approach are introduced as follow:

1. Initializes the state variables and system parameters of the electricity subsystem and the heat subsystem.
2. Input the real-time measurement data of the IEHN to determine the real-time topology of the heat subsystem.
3. Based on the principle of the minimum number of nodes in the ring-shaped heating network, divide the heat subsystem and determine the boundary constraint.
4. Input system coupling constraints and boundary state constraints.
5. Calculate the measurement equation $h_e(x_e)$ and $h_h(x_h)$. The measurement equation of the thermal model in the radiant partition is replaced by formula (16).

6. Solve the state estimation model (1) by the primal-dual interior point method (PDIPM) [26].
7. Judge whether the results satisfies the convergence condition δ.

5. Simulation Study

The performance of the fast state estimation approach proposed in this paper were tested for a simple case shown in Figure 1 and the Barry Island case shown in Figure 6. The parameters of case study 1 are shown in Appendix A. The detailed parameters of the two cases are presented elsewhere [7].

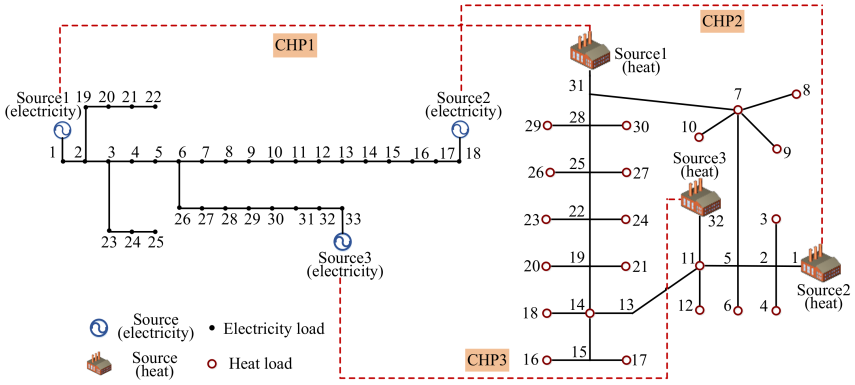

Figure 6. Structure of the Barry Island case (case study 2).

5.1. Accuracy of the State Estimator

This section analyzes the different SE methods through both filtering effect and state variable precision perspectives. Generally, the ratio between measurement error statistics S_H and estimated error statistics S_M is selected to characterize the performance of SE, which are given as follows:

$$\begin{aligned} S_M &= \frac{1}{M}\sum_{j=1}^{M}\left[\frac{1}{N}\sum_{i=1}^{N}\left(\frac{z_{i,t}-h_i(x_{true})}{\sigma_i}\right)^2\right]^{\frac{1}{2}} \\ S_H &= \frac{1}{M}\sum_{j=1}^{M}\left[\frac{1}{N}\sum_{i=1}^{N}\left(\frac{h_{i,t}(x_{se})-h_i(x_{true})}{\sigma_i}\right)^2\right]^{\frac{1}{2}} \end{aligned} \tag{18}$$

where M is the test number, N is the numbers of the measurements and $z_{i,t}$ is generated by the true value adding Gaussian noises with 0.01–0.05 standard deviation in each test, σ_i is the standard deviation of the Gaussian noises, and $h_{i,t}(x_{se})$ is the evaluated value in each test. Smaller ratio of S_H/S_M means the better effects of SE.

Table 1 shows the comparison results of WLS, WLAV and the proposed method (FAST-SE) in two cases under the full measurement system configuration. Each result is obtained by performing 2000 experiments.

Table 1. The comparison of statistical results. WLS: weighted least square; WLAV: weighted least absolute value; FAST-SE.

Case	Algorithm	Power Network			Heating Network		
		S_M	S_H	*Ratio*(%)	S_M	S_H	*Ratio*(%)
1	WLS	0.9901	0.5425	54.79	0.9901	0.5127	51.78
	WLAV	0.9901	0.5574	56.30	0.9898	0.5247	53.01
	FAST-SE	0.9901	0.5573	56.29	**0.9900**	**0.5250**	**53.03**
2	WLS	0.9966	0.4439	44.54	0.9924	0.3538	35.65
	WLAV	0.9966	0.5245	52.62	0.9924	0.3719	37.47
	FAST-SE	0.9966	0.5249	52.66	**0.9924**	**0.3797**	**38.26**

It can be seen from Table 1 that the minimum ratio S_H/S_M of WLS means that its overall estimation accuracy is the highest among the three algorithms. And the state estimator results of WLAV and FAST-SE are very close to that of WLS. In addition, in the large and small case tests, the estimation accuracy of FAST-SE is almost the same as that of WLAV. So, we can draw the conclusion that the approximate model of radiant heating network has little effect on the accuracy of state estimation results.

The local accuracy of state estimation results is evaluated by the average relative error:

$$e_x(\%) = \frac{100}{M}\sum_{J=1}^{M}\left(\frac{1}{N}\sum_{i=1}^{N}\left|\frac{x_{i,t}-x_{true}}{x_{true}}\right|\right)\times 100\% \tag{19}$$

Figures 7–9 show the average relative error of state variables x_h in the heat subsystem under 2000 experiments. It can be seen from the line chart in Figure 7 that only a few nodes have a slightly larger average error, and the error of return temperature is basically consistent with WLAV. Taking the estimated value of WLS (histogram) as a comparison benchmark, we can see that the local estimation accuracy of the state quantity of FAST-SE and WLAV can be controlled within 0.4%, which meets the accuracy requirements of state estimation.

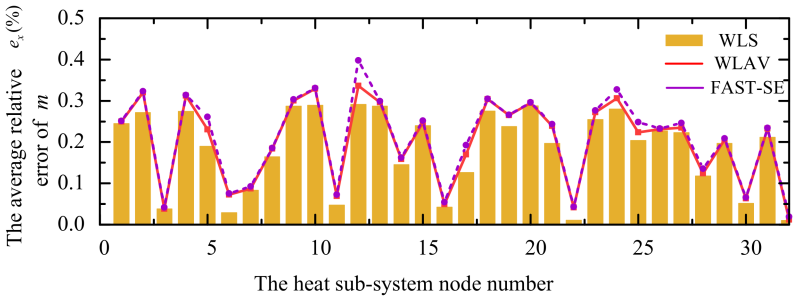

Figure 7. The average relative error $e_x(\%)$ of m.

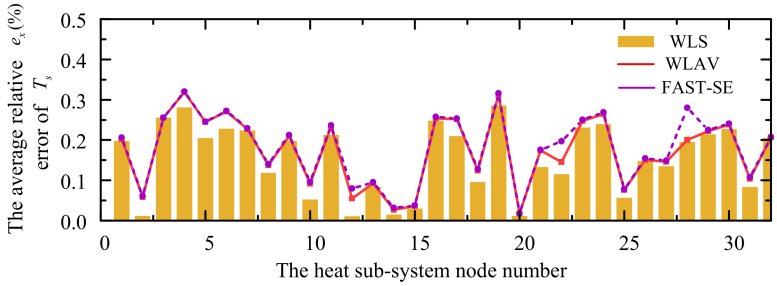

Figure 8. The average relative error $e_x(\%)$ of T_s.

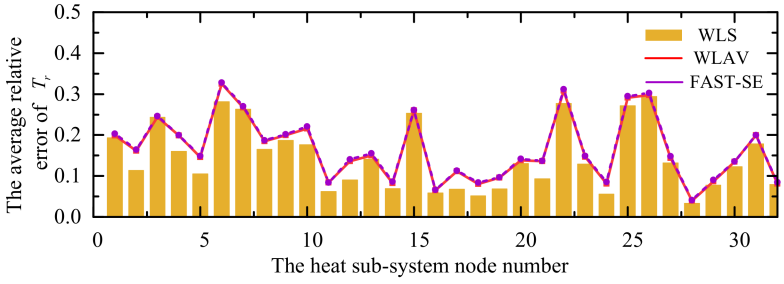

Figure 9. The average relative error $e_x(\%)$ of T_r.

Through the above two tests, it can be concluded that the fast state estimation method proposed in this paper is similar to WLAV in accuracy.

5.2. Computational Efficiency of the State Estimator

Under the conditions of an Intel i5-8250u processor, the computational efficiency test was carried out. The comparison of the computational time and iterations of the three state estimators under large and small system scales is shown in Table 2. It can be seen from Table 2 that the method presented in this paper has obvious advantages in computing efficiency in IEHN without a ring-shaped heating network (case study 1). Compared with WLAV, the computational efficiency of the method proposed in this article is increased by more than 60%. Due to the simplification of the temperature drop equation in the radiant heating network, the constantization of some elements of the Jacobian matrix during the iteration process improves the computational efficiency.

Table 2. The comparison of computational efficiency.

Case	Algorithm	Computational Time	Iterations
1	WLS	0.0466 s	4
	WLAV	0.0652 s	12
	FAST-SE	**0.0173 s**	**6**
2	WLS	0.0874 s	5
	WLAV	0.1822 s	13
	FAST-SE	**0.0693 s**	**8**

Figure 10 shows the computational performances of case study 2 obtained under 2000 experiments. It can be seen from the figure that the computational efficiency of the method presented in this paper is much higher than that of WLAV. And the computation time and convergence times of FAST-SE is close to WLS. Since the computational efficiency is mainly restricted by the numerical stability of the heat subsystem, the calculation scale of ring-shaped heat network is greatly reduced by partition and the convergence times of radiant heating network are very low.

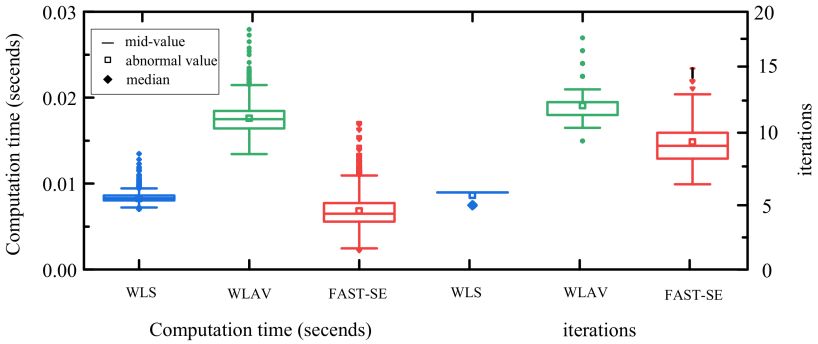

Figure 10. The comparison of computational performances.

6. Conclusions

In order to solve the computational efficiency and numerical stability of the robust estimation method of the electric-heat interconnected system, this paper proposes a fast state estimation method for the electric-heat interconnected system based on WLAV. From the perspective of simplification and distribution of the heating network model, this method decouples the ring heating network and the radial heating network through heating network partitions and increases boundary constraints, reducing the overall calculation scale. By comparing with the existing WLS and WLAV algorithms, the proposed method is almost the same as WLAV in accuracy, but it has a great improvement in computational efficiency, which is very important for a robust estimator. It should be noted that future IEHN-SE research will focus on the application of energy unified model research. At the same time, how to improve the state estimation technology to realize the accurate and rapid tracking of the system in the situation of system disturbance is also one of the research topics.

Author Contributions: Conceptualization, investigation and writing-original draft preparation, C.W. and M.G.; methodology, Q.X.; software and formal analysis, H.Z.; validation, Q.X.; writing-review and editing M.G., funding acquisition, Q.X. All authors have read and agreed to the published version of the manuscript.

Funding: This work was supported in part by the Science and Technology Project of SGCC under grant SGJSJX00YJJS1800721.

Acknowledgments: The completion of this paper has been helped by many teachers and classmates. We would like to express our gratitude to them for their help and guidance.

Conflicts of Interest: The authors declare no conflict of interest.

Nomenclature

A. Index

IEHNs	integrated electrical and heating networks
SE	state estimation
WLS	weighted least square
WLAV	weighted least absolute value
N_e^{meas}	set of the measurements in eps

b. constant and coefficient

Y	node admittance matrix of electricity subsystem
B	loop-branch incidence matrix
K	pipe resistance coefficient
A_k	node-branch incidence matrix
ζ	coupling coefficient of CHP

c. variables

x_e	state variables of electricity subsystem
x_h	state variables of heat subsystem
$h_e(x_e)$	measurement functions of electricity subsystem
T_a	the ambient temperature
$h_h(x_h)$	measurement functions of heat subsystem
z_e	measurements vector of electricity subsystem
z_h	measurements vector of heat subsystem
w_e,w_h	error variances columns of the measurements in the electricity subsystem and the heat subsystem
P_{ij}^{meas}	measurements of branch active power ij
Q_{ij}^{meas}	measurements of branch reactive power ij
P_i^{meas}	measurements of active injection power at node i
Q_i^{meas}	measurements of reactive injection power at node i
V_i^{meas}	measurements of voltage magnitude at node i
m^{meas}	measurements of mass flow rates
m_q^{meas}	measurements of mass flow rates injected
h_f^{meas}	measurements of head losses
Φ^{meas}	measurements of heat power
T_s^{meas}	measurements of supply temperature
T_r^{meas}	measurements of return temperature
T_s',T_r'	the difference between supply / return temperature and the ambient temperature
T_o	outlet temperature before to mixing in the return network
P_{CHP}	power generated by CHP

Appendix A. Parameters of Case Study 1

Electricity Network
The base power is 1MVA and the base voltage is 11kV.
Voltage magnitude of the sources are: $\|V_{1,source}\|$ = 1.05 p.u., $\|V_{2,source}\|$ = 1.02 p.u.
Voltage angle of Source 2 at busbar 4 is: $\theta_4 = 0°$.
Active power of each load are: $P_{1,load} = P_{2,load}$ = 0.15 MW.
Power factor of each load is: cosΦ = 0.95.
Impedance of each line is: Y = 0.09 + j0.1577p.u.
Heating Network
$\Phi_{1,load} = \Phi_{2,load} = \Phi^{3,load}$ = 0.3 MW.
$T_{s1,source}$ = 100 °C, $T_{o1,load} = T_{o2,load} = T_{o3,load}$ = 50 °C.
Ambient temperature is: Ta = 10 °C.
The parameters of each pipe are: D = 0.15 m, $\varepsilon = 1.25 \times 10^{-3}$ m, λ = 0.2 W/mK, L = 400 m.
Water density is: ρ = 958.4 kg/m3. Cp = 4182 J/(kg·K)) = 4.182×10^{-3} MJ/(kg·K)).

References

1. Huang, A.Q.; Crow, M.L.; Heydt, G.T.; Zheng, J.P.; Dale, S.J. The Future Renewable Electric Energy Delivery and Management (FREEDM) System: The Energy Internet. *Proc. IEEE* **2011**, *99*, 133–148. [CrossRef]
2. Gu, W.; Wu, Z.; Bo, R.; Liu, W.; Zhou, G.; Chen, W.; Wu, Z. Modeling, planning and optimal energy management of combined cooling, heating and power microgrid: A review. *Int. J. Electr. Power Energy Syst.* **2014**, *54*, 26–37. [CrossRef]
3. Geidl, M.; Andersson, G. Optimal power flow of multiple energy carriers. *IEEE Trans. Power Syst.* **2007**, *22*, 145–155. [CrossRef]
4. Jia, H.; Wang, D.; Xu, X.; Yu, X.D. Research on some key problems related to integrated energy systems. *Autom. Electr. Power Syst.* **2015**, *39*, 198–207.
5. Wu, J.; Yan, J.; Jia, H.; Hatziargyriou, N.; Djilali, N.; Sun, H. Integrated Energy Systems. *Appl. Energy* **2016**, *167*, 155–157. [CrossRef]
6. Chen, Q.; Hao, J.; Zhao, T. An alternative energy flow model for analysis and optimization of heat transfer systems. *Int. J. Heat Mass Transf.* **2017**, *108*, 712–720. [CrossRef]
7. Liu, X.; Wu, J.; Jenkins, N.; Bagdanavicius, A. Combined analysis of electricity and heat networks. *Appl. Energy* **2016**, *162*, 1238–1250. [CrossRef]
8. Zang, H.; Cheng, L.; Ding, T.; Cheung, K.W.; Wei, Z.; Sun, G. Day-ahead photovoltaic power forecasting approach based on deep convolutional neural networks and meta learning. *Int. J. Electr. Power Energy Syst.* **2020**, *118*, 105790. [CrossRef]
9. Li, Z.; Wu, W.; Wang, J.; Zhang, B.; Zheng, T. Transmission-Constrained Unit Commitment Considering Combined Electricity and District Heating Networks. *IEEE Trans. Sustain. Energy* **2016**, *7*, 480–492. [CrossRef]
10. Chen, S.; Wei, Z.; Sun, G.; Cheung, K.W.; Wang, D.; Zang, H. Adaptive Robust Day-Ahead Dispatch for Urban Energy Systems. *IEEE Trans. Ind. Electron.* **2019**, *66*, 1379–1390. [CrossRef]
11. Li, R.; Wei, W.; Mei, S.; Hu, Q.; Wu, Q. Participation of an Energy Hub in Electricity and Heat Distribution Markets: An MPEC Approach. *IEEE Trans. Smart Grid* **2019**, *10*, 3641–3653. [CrossRef]
12. Chen, S.; Wei, Z.; Sun, G.; Cheung, K.W.; Sun, Y. Multi-linear probabilistic energy flow analysis of integrated electrical and natural-gas systems. *IEEE Trans. Power Syst.* **2017**, *32*, 1970–1979. [CrossRef]
13. Fang, T.; Lahdelma, R. State estimation of district heating network based on customer measurements. *Appl. Therm. Eng.* **2014**, *73*, 1211–1221. [CrossRef]
14. Dong, J.; Guo, Q.; Sun, H.; Pan, Z. Research on state estimation for combined heat and power networks. In Proceedings of the IEEE Power and Energy Society General Meeting (PESGM), Boston, MA, USA, 17–21 July 2016.
15. Sheng, T.; Guo, Q.; Sun, H.; Pan, Z.; Zhang, J. Two-stage State Estimation Approach for Combined Heat and Electric Networks Considering the Dynamic Property of Pipelines. *Energy Procedia* **2017**, *142*, 3014–3019. [CrossRef]

16. Zhang, T.; Li, Z.; Wu, Q.; Zhou, X. Decentralized state estimation of combined heat and power systems using the asynchronous alternating direction method of multipliers. *Appl. Energy* **2019**, *248*, 600–613. [CrossRef]
17. Zang, H.; Geng, M.; Xue, M.; Mao, X.; Huang, M.; Chen, S.; Wei, Z.; Sun, G. A Robust State Estimator for Integrated Electrical and Heating Networks. *IEEE Access* **2019**, *7*, 109990–110001. [CrossRef]
18. Chen, Y.; Zheng, S.; Yang, N.; Lang, Y. Bilinear robust state estimation method for integrated electricity-heat energy systems. *Electr. Power Autom. Equip.* **2019**, *39*, 47–54.
19. Sheng, T.; Yin, G.; Guo, Q.; Sun, H.; Pan, Z. A Hybrid State Estimation Approach for Integrated Heat and Electricity Networks Considering Time-scale Characteristics. *J. Mod. Power Syst. Clean Energy* **2020**, *8*, 636–645. [CrossRef]
20. Zheng, W.; Li, Z.; Liang, X.; Zheng, J.; Wu, Q.H.; Hu, F. Decentralized State Estimation of Combined Heat and Power System Considering Communication Packet Loss. *J. Mod. Power Syst. Clean Energy* **2020**, *8*, 646–656. [CrossRef]
21. Chen, Y.; Zheng, S.; Yang, N.; Yang, X.; Liu, K. Robust State Estimation of Electric-Gas Integrated Energy System Based on Weighted Least Absolute Value. *Autom. Electr. Power Syst.* **2019**, *43*, 1000–1026.
22. Zheng, S.; Liu, J.; Chen, Y.; Qi, B. Bilinear Robust State Estimation Based on Weighted Least Absolute Value for Integrated Electricity-gas System. *Power Syst. Technol.* **2019**, *43*, 3733–3744.
23. Gomez-Exposito, A.; Gomez-Quiles, C.; Jaen, A.D.L.V. Bilinear power system state estimation. *IEEE Trans. Power Syst.* **2012**, *27*, 493–501. [CrossRef]
24. Gol, M.; Abur, A. LAV Based Robust State Estimation for Systems Measured by PMUs. *IEEE Trans. Smart Grid* **2014**, *5*, 1808–1814. [CrossRef]
25. Sun, G.; Wang, W.; Wu, Y.; Hu, W.; Jing, J.; Wei, Z.; Zang, H.I. Fast Power Flow Calculation Method for Radiant Electric-Thermal Interconnected Integrated Energy System. *Proc. Chin. Soc. Electr. Eng.* **2020**, *20*, 436–443.
26. Wei, H.; Sasaki, H.; Kubokawa, J.; Yokoyama, R. An interior point method for power system weighted nonlinear L-1 norm static state estimation. *IEEE Trans. Power Syst.* **1998**, *13*, 617–623. [CrossRef]